FEBS Letters

journal homepage: www.FEBSLetters.org

Review

Cytochrome *c* oxidase: Intermediates of the catalytic cycle and their energy-coupled interconversion

Alexander A. Konstantinov *

A.N. Belozersky Institute, Moscow State University, Moscow 119991, Russia

ARTICLE INFO

ABSTRACT

Several issues relevant to the current studies of cytochrome *c* oxidase catalytic mechanism are discussed. The following points are raised. (1) The terminology currently used to describe the catalytic cycle of cytochrome oxidase is outdated and rather confusing. Presumably, it would be revised so as to share nomenclature of the intermediates with other oxygen-reactive heme enzymes like P450 or peroxidases. (2) A "catalytic cycle" of cytochrome oxidase involving complete reduction of the enzyme by 4 electrons followed by oxidation by O_2 is a chimera composed artificially from two partial reactions, reductive and oxidative phases, that never operate together as a true multi-turnover catalytic cycle. The $4e^-$ reduction–oxidation cycle would not serve a paradigm for oxygen reduction mechanism and protonmotive function of cytochrome oxidase. (3) The foremost role of the K-proton channel in the catalytic cycle may consist in securing faultless delivery of protons for heterolytic O–O bond cleavage in the oxygen-reducing site, minimizing the danger of homolytic scission reaction route. (4) Protonmotive mechanism of cytochrome oxidase may vary notably for the different single-electron steps in the catalytic cycle.

© 2011 Federation of European Biochemical Societies. Published by Elsevier B.V.

1. Introduction

Cytochrome *c* oxidase (COX) is a terminal enzyme of the respiratory chain of mitochondria and many bacteria and a key enzyme of aerobic respiration. The enzyme is plugged through the coupling membrane of mitochondria or bacteria and catalyses reduction of molecular oxygen to water. The free energy of the reaction is transduced to transmembrane difference of proton electrochemical potential, $\Delta\mu H^+$:

$$4\text{cyt } c^{2+} + O_2 + 8H_{in}^+ = 4\text{cyt } c^{3+} + 2H_2O + 4H_{out}^+ + 8q^+ \uparrow \quad (1)$$
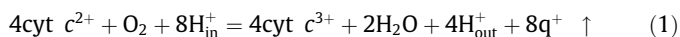
where $8q^+\uparrow$ denotes net translocation of 8 positive charges across the coupling membrane from the inner negatively charged (*N*) to the outer positively charged (*P*) aqueous phase. Four charges cross the membrane because of anisotropic (vectorial) chemistry of the process, as the 4 electrons coming from cytochrome *c* at the outer *P*-side of the membrane combine with four "chemical" protons taken up from the inner *N*-aqueous phase in order to reduce

O_2 to $2H_2O$. Four charges more are translocated from the *N*- to the *P*-side of the membrane by virtue of proton pumping coupled to the reaction chemistry. In some bacterial oxidases the number of pumped protons (and hence the overall number of charges translocated) may be less than in the mitochondrial cytochrome *c* oxidase and its bacterial homologues.

The enzyme has been studied in great detail (see [1–4] for excellent recent reviews) and the protonmotive function of cytochrome oxidase with its vectorial chemistry coupled to proton pumping became a model paradigm in the studies of the molecular mechanism of energy transduction by the membrane-bound redox enzymes. In order to understand how COX conserves free energy of O_2 reduction for generation of $\Delta\mu H^+$, it is important to resolve the complex catalytic cycle of the enzyme into intermediate steps and to explore the molecular mechanism of energy transduction at each of the steps.

Cytochrome *c* oxidase contains 4 redox-active metal centers. The electron transfer sequence can be described by a simple scheme:

$$\text{cyt } c \rightarrow Cu_A \rightarrow \text{heme } a \rightarrow [\text{heme } a_3, \; Cu_B] \rightarrow O_2 \quad (2)$$

where heme a_3 iron and "invisible" ion of Cu_B located within $\sim$4.5 Å from each other form a dioxygen reducing site, often referred as "binuclear center" (BNC). In this center, heme iron serves primarily as an anchor oxygen during O_2 reduction as well as an immediate donor of the 1st, 3rd and 4th electrons to the bound O_2, whereas

Cu_B operates as a redox-regulated gate for passage of oxygen dissolved in the membrane into the heme a_3/Cu_B cavity, and also serves as a donor of one of the two electrons (the second one) required for reduction of heme a_3^{2+}-bound oxygen to bound peroxide, as well as an acceptor for the OH^-/H_2O formed upon heterolytic splitting of the bound peroxide. This review goes briefly over a few selected issues in the current studies of the cytochrome oxidase mechanism which seem important to me.

2. Catalytic cycle intermediates

A catalytic cycle of cytochrome oxidase is outlined in Fig. 1. To begin with, some comments are due regarding the terminology.

2.1. Nomenclature of the intermediates

The set of the names and abbreviations currently used to denote the catalytic intermediates of COX is regretfully outdated although still retained "for historical reasons", which may be very confusing for a reader who is not in the picture of the history of the COX studies. I remember how Antonio Xavier complained to me about illogical system of abbreviations used in the cytochrome oxidase literature. A description of the catalytic cycle of COX in the current literature may look like following:

$$O \rightarrow R^2 \rightarrow A_M \rightarrow P_M \rightarrow F \rightarrow O \qquad (3)$$

or

$$O \rightarrow R^4 \rightarrow A_R \rightarrow P_R \rightarrow F \rightarrow O \qquad (4)$$

for the reactions passing via the 2- (R^2) and 4-electron reduced states (R^4), respectively. There are at least two apparent flaws inherent in the terminology.

First, while **O, R, P, F** are single-letter abbreviations for trivial names of different redox states (**O**xidized, **R**educed, **P**eroxy, **F**erryl, respectively), the **A** denoting the oxygenated complex of ferrous heme a_3 is borrowed from the intermediate series **A, B** and **A, C** described by Chance and coworkers long ago [5]. Hence, **A** is obviously an alien in the sequences (3) and (4). (A recent attempt to correct the situation by re-interpreting **A** as an abbreviation for **Ad**duct [6] is appreciated!). An abbreviation **Oxy** is used sometimes to denote the oxycomplex but it contains 3 letters while **O** is already in use for the oxidized form. It is then noted, that the oxycomplex of heme a_3^{2+} is actually a resonance mixture [ferrous-**Oxy** ↔ ferric-**S**uperoxo], where the ferric-superoxo state is the dominating species ([7–10]). Therefore, an abbreviation **S** can be offered to replace **A** in description of COX catalytic cycle (Fig. 1).

Second, the abbreviation **P** (peroxy) still used to denote the compounds which are not at all peroxy as believed some 30 years ago [5,11] is fully outdated and misleading, which is further aggravated by the fact that the two "peroxy" intermediates "P_M" and "P_R" are at different redox levels of the binuclear center. As a matter of fact, the intermediates "P_M" and **F** formed after cleavage of the O–O bond in the ferric-peroxy state of COX, are equivalent to the ferryl-oxo Compounds I and II of peroxidases, respectively [4,9,12], while "P_R" is simply an underprotonated form of **F** (Compound II), rather than a homologue of "P_M" (Compound I). Abbreviations F_I and F_{II} may be suggested for the two consecutive **F**erryl states of heme a_3 [12,13], where the subscripts I and II
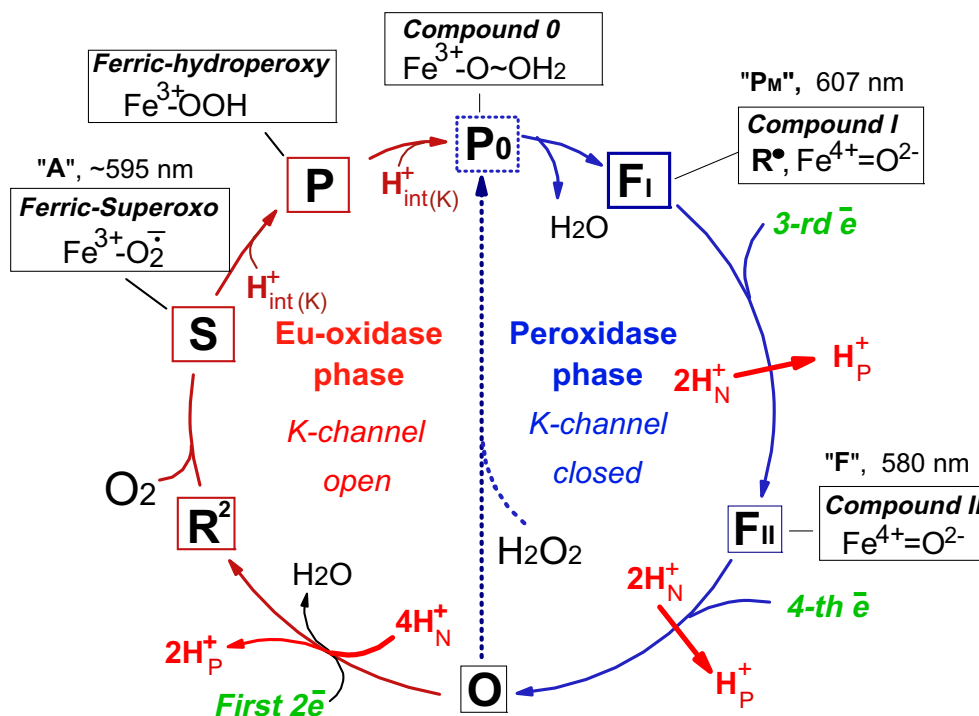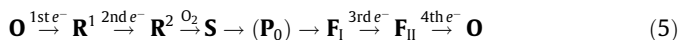

Fig. 1. Catalytic cycle of cytochrome c oxidase. The cycle going through the 2 electron reduced state is modified from the schemes in [12,61]. The intermediates at the peroxy level of heme a_3 (**P**, ferric-hydroperoxy, and P_0, ferric-dihydroperoxy) have not yet been observed experimentally, hence shown in dotted boxes. They are homologous to the intermediates of P450 and peroxidases [7,20,108] and are considered in theoretical models of the O–O bond splitting in cytochrome oxidase [9,18,19,109]. Ferric-hydroperoxy complex of heme a_3 has been trapped very recently during catalytic turnover of synthetic model of COX at low temperatures [48]. The singly-reduced R^1 state as well as the unprotonated ferric-peroxo intermediate (Fe^{3+}–O–O^-) formed on a way from **S** to **P** have been omitted for simplicity. The two internal protons required for generation of P_0 and heterolytic cleavage of the O–O bond may be borrowed from the binuclear center terminus of the K-proton channel via the water molecule(s) inside the heme cavity that equilibrate protonically with the K-channel via the OH group of $Tyr244_{bt}$ [9,12,55,61] (see the text). These protons are denoted as $H^+_{int(K)}$ to distinguish them from the protons taken up all the way from the N-bulk aqueous phase (H^+_N). Description of the proton pumping events in the euoxidase half of the catalytic cycle is complicated by existence of multiple forms of the oxidized and singly-reduced forms of the enzyme, with differences among them not yet understood (cf. section 3.1). Therefore, working out in detail the individual proton pumping steps in this part of the cycle would be premature (see [1,4] for possible mechanisms).

indicate homology of the two ferryl intermediates to the Compounds I and II of peroxidases as well as the order of their appearance in the catalytic cycle of COX (Fig. 1). Accordingly, a subscript 0 is added to $\mathbf{P}$ in case of the ferric-dihydroperoxy complex of heme a_3 to emphasize homology of the intermediate to Compound 0 of peroxidases formed transiently upon H_2O_2 binding with the ferric heme iron. The catalytic cycle passing through the $2e^-$-reduced state may then be depicted, omitting some details, by a scheme:

$$\mathbf{O} \xrightarrow{1st\,e^-} \mathbf{R}^1 \xrightarrow{2nd\,e^-} \mathbf{R}^2 \xrightarrow{O_2} \mathbf{S} \rightarrow (\mathbf{P}_0) \rightarrow \mathbf{F}_I \xrightarrow{3rd\,e^-} \mathbf{F}_{II} \xrightarrow{4th\,e^-} \mathbf{O} \qquad (5)$$

2.2. The catalytic cycles running via the $2e^-$- and $4e^-$-reduced state of COX

As noted above, there are two kinds of cytochrome oxidase catalytic cycle commonly considered in the literature in which the enzyme passes through the $4e^-$- or $2e^-$-reduced state. Under anaerobic conditions, the oxidized enzyme can be fully reduced by four electrons ($\mathbf{O} + 4e^- \rightarrow \mathbf{R}^4$) with a strong chemical reductant like dithionite in vitro or, in vivo, by the low-potential respiratory substrates in anoxic tissues, and the fully-reduced enzyme can be oxidized by O_2 via a number of intermediates back to the oxidized state ($\mathbf{R}^4 \rightarrow \mathbf{A}_R \rightarrow \mathbf{P}_R \rightarrow \mathbf{F} \rightarrow \mathbf{O}$). These two half-reactions reactions can be put together on paper to form a cycle (Eq. (4)), composed of the reductive and oxidative phases. However, such a cycle is in fact no more than a chimera, an artificial sum of two partial reactions, and is not *catalytic*. That is, under no realistic conditions can it run multiple turnovers on a steady-state basis, which is a compulsory requirement for catalysis. In the respiratory chain, COX receives electrons from cytochrome c one by one, and electron supply from the cytochrome chain is much slower (say, $10\,s^{-1}$ or less) than oxidation of the binuclear site by O_2 ($k_v > 10^8\,M^{-1}\,s^{-1}$, i.e. at least $10^2\,s^{-1}$ at O_2 concentration as low as $1\,\mu M$). Therefore under aerobic conditions, as soon as COX receives the first two electrons it will be immediately oxidized by O_2 to Compound I ($\mathbf{F}_I$, "$\mathbf{P}_M$") before any further reduction of the enzyme can occur. Hence, "the fully reduced enzyme is, as such, a very improbable state during turnover under physiological conditions" [4].

At the same time, oxidation of the fully reduced COX by oxygen followed by various time-resolved measurements (absorption, EPR, RR and FTIR spectroscopy of the enzyme, proton uptake/release, electrometric measurements of charge translocation across the membrane etc.) is a convenient and powerful experimental tool, amply used in the studies of the dioxygen reduction mechanism (reviewed, [1,4,14,15]). However, since the mechanism of the O–O bond cleavage when starting from the fully reduced state is not the same as during oxidation of the two-electron reduced form, the intermediates formed during oxidation of the fully reduced COX (at least some of them, like "$\mathbf{P}_R$") may not be identical to the intermediates involved in the normal catalytic cycle (cf. [16]), and discussion of these results is minimized in this paper *ex proposito*.

Fig. 1 outlines a catalytic cycle passing through the $2e^-$-reduced state (Eq. (3)), which may be more or less relevant to physiological conditions. Whereas the artificial cycle through the fully reduced state (Eq. (4)) contains distinct phases of reduction and oxidation, it is not the case with the cycle going through the $2e^-$ reduced state. It is difficult to understand why *reduction* of COX by the 3rd and 4th electrons would be referred as an *oxidative* phase as often found in the literature (e.g., [17]). At the same time, the two halves of the cycle in Fig. 1 represent two easily recognizable reactions found in P450s and peroxidases.

In the first half, the oxidized enzyme receives sequentially 2 electrons from cytochrome c which enter eventually the oxygen-reducing site. Oxygen pathway form the hydrophobic membrane milieu to the intraprotein heme a_3 cavity lies through a special oxygen channel which is plugged up at the end by Cu_B. Molecular oxygen does not react with the oxidized copper, Cu(II), but readily binds Cu(I). Therefore, reduction of Cu_B by one of the first two electrons received by the BNC opens a gate for O_2 passage from the oxygen channel, via transient weak binding to Cu_B^{1+} and into the heme cavity, where it is anchored finally by heme a_3^{2+} and a ferric-superoxide complex ($\mathbf{S}$) is formed. Subsequently Cu_B^{1+} will donate its electron together with a proton from a near by water molecule [9,12,18,19] to the Fe(III)-superoxide complex $\mathbf{S}$ of heme a_3 reducing it to Fe(III)-hydroperoxy state, $\mathbf{P}$, analogous to the iron-hydroperoxy intermediate of P_{450} [7,20], and addition of the second proton converts $\mathbf{P}$ to $\mathbf{P}_0$. The part of the cycle from $\mathbf{O}$ to $\mathbf{P}_0$ may be denoted as "euoxidase" phase of the cycle [12]) because it includes $2e^-$ reduction of the enzyme followed by its $2e^-$ oxidation by molecular oxygen to (bound) H_2O_2, which is a typical oxidase reaction in enzymology.

Subsequent events follow a pattern typical of peroxidase reaction. As soon as the second proton is added to Fe(III)-hydroperoxy complex, the O–O bond in the unstable dihydroperoxy intermediate, Fe(III)-O$\sim$OH$_2$ is cleaved *heterolytically* [9,12,18,19]. The distal oxygen atom cleaves off with 2 extra electrons and 2 protons and forms the first H_2O molecule which can coordinate to Cu_B^{2+} (e.g., as OH$^-$) [1,4] or make a hydrogen bond to Tyr244$_{bt}$ [9,21]. The second oxygen atom (oxene) that is an extremely strong oxidant remains tightly bound to heme a_3 iron and converts to O^{2-} ion, equivalent to doubly deprotonated water, withdrawing one electron from Fe(III) and one more from some near by aromatic residue (perhaps via transient formation of the porphyrin ring π-cation radical that is re-reduced rapidly by some near by aromatics). As a result, Compound I-type ferryl-oxo intermediate $\mathbf{F}_I$ is formed. The flawless heterolytic splitting of the O–O bond may be a crucial step in the entire O_2 reduction cycle, since even minor deviations in the reaction profile can lead to homolytic scission of the O–O band and formation of an extremely harmful hydroxyl radical at BNC with high probability of oxidative destruction of the porphyrin ring of heme a_3.

Both protons required for splitting of the O–O bond are likely to be borrowed from the BNC terminus of the K-proton channel via a hydrogen bond network consisting of an H_2O trapped between His240$_{bt}$ and Tyr244$_{bt}$, Tyr244 phenolic group, and OH group of the hydroxyethylfarnesyl substituent in heme a_3 hydrogen bonded via H_2O to Tyr316$_{bt}$ [9,18,19,21,22]. Therefore, the exergonic splitting of the O–O bond may provide a driving force for proton uptake via the K-channel. Securing faultless delivery of protons required for heterolytic cleavage of the O–O bond may constitute the primary and most important functional role of the K-channel.

3. Some specific comments on the intermediates

3.1. Oxidized state

3.1.1. Multiple forms

There is considerable uncertainty concerning the structure of the binuclear site in the oxidized COX. That the oxidized form of COX can exist in multiple states differing in catalytic, redox, spectral and ligand-binding characteristics has been long known: fast/slow, alkaline/acidic, pulsed/resting, oxygenated, Cl-bound, CO$_2$-bound, "recently oxidized" and $\mathbf{O}_H$ forms can be mentioned [1,23]. Structural and physico-chemical differences among these states are not well understood, but protonation state of His-Tyr244$_{bt}$ phenolic group with pK $\sim$ 6.8 [24] is definitely important [25]. Although crystal structure of the oxidized COX has been solved at high resolution for the mitochondrial and bacterial enzyme ([22,26,27] and references therein), the crystals are obtained at pH well below 7, while the "fast" form of the enzyme requires

that pH is kept at 8 or higher. Therefore, the 3D-structure of the oxidized COX likely corresponds to the acidic "slow" form of the enzyme with Tyr244$_{bt}$ protonated, and we do not know the structure of BNC in the active form of the enzyme for which most of the experimental work has been performed. The chloride- and CO$_2$-bound forms of the mitochondrial oxidase [23,28] though not identified yet by crystal structure analysis, may be of physiological significance. Notably, Cl$^-$ ion fits ideally the space between heme a_3 iron and Cu$_B$ in the crystal structure of the oxidized COX ([27,29] and references therein).

3.1.2. Is there peroxide bound in the active site of the oxidized enzyme?

The crystal structure of the oxidized A-class oxidase (see [30] for classification) from either mitochondria or bacteria reveals electron density between heme a_3 iron and Cu$_B$ corresponding to the presence of two oxygen atoms [22,27,29,31]. The same feature has been revealed recently in the BNC of B-class ba_3 oxidase from *T. thermophilus* [32]. According to analysis of the crystal structure [26,27,31,32] corroborated by RR spectroscopy data [33], the atoms may belong to peroxide dianion bridging heme a_3^{3+} iron and Cu$_B^{2+}$. As proposed in [26], the bridging peroxide may be a distinctive feature of the "resting" COX, as opposed to the "recently oxidized" enzyme (e.g., **O**$_H$, see below) with heme a_3 in the Fe^{3+}-OH$^-$ state [34,35]. The distance of 1.6–1.7 Å between the two oxygen atoms reported for the A-class oxidases [26,27,31] is somewhat longer than the ~1.5 Å expected for peroxide, but in the ba_3 oxidase the bond length is close to 1.5 Å [32]. At variance with the above works, analysis of the crystal structures and theoretical modeling in [10] led to conclusion that the 2 oxygen atoms in the binuclear site are better explained by superoxide bound to ferric heme a_3 (though the O–O bond in superoxide has to be even shorter than 1.5 Å). The peroxide or superoxide may be formed in the binuclear site during collection of the data due to reduction by synchrotron radiation.

3.1.3. O$_H$-state

Immediately after oxidation of the fully reduced COX from mitochondria or several bacterial species by molecular oxygen, a metastable form of the oxidized enzyme is formed denoted as **O**$_H$ [36–39] that is functionally different from the resting oxidized state **O**. At this time it remains unknown whether the **O**$_H$ state is formed under any conditions other than oxidation of the fully reduced oxidase, e.g. upon single-electron reduction of Compound II (**F**$_{II}$) to **O**. There are two diagnostic features of **O**$_H$: (1) upon single-electron photoreduction of the intermediate, the electron goes rapidly from the low-spin heme a to Cu$_B$ as the final acceptor; (2) this ET is coupled to transmembrane proton pumping and uptake of a chemical proton from the *N*-phase. In contrast, upon single-electron reduction of the "resting" oxidized form (even in the "fast" preparations), the electron received by Cu$_A$ is transferred rapidly to heme a (heme b in ba_3 oxidase), but subsequent ET to the binuclear site is (*i*) slow as compared to turnover number of the enzyme [40,41] and (*ii*) the electron goes to heme a_3 rather than Cu$_B$ [37], as shown most clearly for the ba_3 oxidase [38]. Moreover, this slow ET is not coupled to proton pumping but only to proton uptake via the K-channel required to charge compensate reduction of heme a_3 [41]. The **O**$_H$ state relaxes spontaneously to the **O** state on a tens of seconds time scale [36]. Little if any is known about the differences in physico-chemical characteristics of the two oxidized forms. The **O**$_H$ and **O** states do not reveal any differences in the absorption or EPR spectra [42] but in all probability, E$_m$ of Cu$_B$ in "**O**$_H$" is much higher than in **O** [37–39]. As argued by Yoshikawa and collaborates [21,43], trigonal planar coordination of Cu$_B$ in the reduced oxidase is very stable which makes Cu$_B^{2+}$ a poor electron donor with high E$_m$. Binding of a strong axial ligand like hydroxide to the oxidized Cu$_B$ upon oxidation of the reduced COX may tend to distort the coordination sphere to a tetrahedral form with lower E$_m$ (the ~+0.35 V value determined by

equilibrium redox titrations [1]); unfortunately, there is no crystal structure available for the oxidized state of the "fast" form of the oxidase due to low pH at which the crystals are obtained. It can be suggested that after oxidation of COX by O$_2$, Cu$_B$ may retain for a while trigonal planar coordination stabilizing the reduced state and hence the high E$_m$ form of the redox-center. Subsequent slow relaxation of coordination sphere of Cu$_B$ to fit the oxidized state of the metal ion could be responsible for the O$_H$ → O transition.

3.2. Reduced state

Crystal structure is available for the fully reduced cytochrome oxidase (state **R**^{4}) [22,43,44] but presumably the structure of BNC and its surroundings should be the same in the **R**^{2} form. There are two features of the **R**-state structure to be underscored: (1) the absence of H$_2$O/OH$^-$ ligands at heme a_3 or Cu$_B$ and (2) the opened gate for water/protons from the K-channel to the BNC reactor cavity, the gate being closed in the oxidized state by a strong hydrogen bond between the OH groups of Tyr244$_{bt}$ and hydroxyethylfarnesyl side chain in the porphyrin ring of heme a_3 [22,43]. Hence the enzyme is prepared to bind O$_2$ and, following two-electron reduction of the bound O$_2$ by a$_3$/Cu$_B$, to recruit protons from the K-channel required for cleavage of the O–O bond.

3.3. Oxycomplex

The electronic configuration of the oxycomplex of heme a_3 is best described as ferric-superoxide [8–10,12,21] (Fig. 1). The crystal structure of the oxycomplex of COX is not available, but the structure of the reduced enzyme complexes with O$_2$ analogs, such as CO, NO and CN$^-$ has been used to deduce characteristics of the oxycomplex [21,43]. According to this reasoning, the heme a_3-bound oxygen in the oxycomplex of the reduced COX may be relatively well isolated from interaction with either Cu$_B$ or Tyr244$_{bt}$ which prevents uncontrolled delivery of the second electron and protons to oxygen in Compound **S** and cleavage of the O–O bond "before the enzyme is prepared for proton pumping" [21]. Reduced Cu$_B$ is likely to form a transient O$_2$ binding site on the way of oxygen from membrane via the oxygen channel and into the a_3/Cu$_B$ cavity as deduced earlier from the CO photodissociation/recombination studies (reviewed, [45]). Transient binding of oxygen to Cu$_B$ in the A-class oxidases is to be weak (it may be stronger in the B-class oxidases like ba_3 from *T. thermophilus* as inferred from the CO binding studies [46]) and may occur in a side-on fashion [21,43]. The protonic/water connection of heme cavity with the K-proton channel observed in the **R** state is retained in the CN$^-$-complexed reduced oxidase [21,22,43].

3.4. Compounds P

The iron-peroxy intermediates of COX have not been observed experimentally but were explored by theoretical modeling. Possible mechanisms of the bound dioxygen reduction to ferric-hydroperoxide and subsequent cleavage of the O–O bond are discussed in [9,18,19,47]. Very recently, formation of the ferric-hydroperoxy complex of heme a_3 has been resolved with a catalytically active biomimetic cytochrome oxidase model at −60 °C [48].

3.5. Compounds I and II

3.5.1. Identity of a free radical in Compound I (**F**$_I$)

Both Compounds I and II of COX contain heme a_3 iron in the ferryl-oxo state. As in the peroxidases, Compound II is single-electron deficient relative to the ferric state **O**, while two electron are required (the 3rd and 4th electrons in the catalytic cycle, Fig. 1) to convert Compound I to the resting oxidized state. Accordingly,

Compound I differs from Compound II by an extra oxidizing equivalent located at some aromatic residue ($R^{\bullet}$ in Fig. 1) close to the binuclear site. This aromatic residue provides the second of the two electrons (the first one is withdrawn from heme a_3 ferric iron converting it to the ferryl state) that are pulled out from the enzyme by the heme a_3 iron-bound oxene atom, formed upon the heterolytic cleavage of the O–O bond in Compound P_0. The identity of this aromatic group has not been firmly established. The problem is complicated by two circumstances: (1) the free radicals close to the metal centers in BNC cannot be easily seen by electron spin resonance spectroscopy; (2) the primary free radical formed can oxidize other nearby aromatic groups giving rise to the secondary radicals. The mainstream opinion attributes the primary radical to the covalently-bound tyrosine $Y244_{bt}$ (reviewed [1,2,4,49]). However, there is increasing evidence in favor of $W236_{bt}$ ($W272_{pd}$) participation in the O–O bond cleavage [50–54], while the role of $Y244_{bt}$ may be reduced to gated proton transfer from the K-channel (cf. the "K-gate" model [55]) via a hydrogen-bonded water molecule ($W510_{bt}$) to the iron-peroxy complex [9]. The primary tryptophan radical $W236_{bt}$ ($W272_{pd}$) can be re-reduced by a near by tyrosine $Y129_{bt}$ ($Y167_{pd}$) or by $Tyr244_{bt}$ giving rise to the secondary tyrosine free radical EPR signals [53,56–58].

3.5.2. The 607/580 nm transition in ferryl-oxo compounds of COX

The absorption maxima of the two ferryl intermediates at ~607 and ~580 nm (in the difference spectra vs the oxidized state) have been long thought to be associated with different redox states of the binuclear center in compounds "**P**" and "**F**", respectively, that appear sequentially in the catalytic cycle. Eventually, it became clear that position of the 607/580 nm absorption maximum is not a specific marker of either Compound I or Compound II of COX, either of which can exist in ~607 or ~580 nm form. The transition from the ~607 to the ~580 nm state in Compound I or Compound II is associated with proton uptake from the bulk phase and protonation of some group in the binuclear site.

Conversion of Compound I (F_I) from the 607 nm to the 575 nm form is induced by lowering pH to ~6 [28,59–62]. The acidic form of F_I characterized by a maximum at 573-576 nm, somewhat shorter than 578-584 nm typical of Compound II, was denoted by Rich as Compound $F^{\bullet}$ ("F dot") [62] to emphasize the presence of free radical(s) in the intermediate. As to Compound II, the $607 \rightarrow 580$ nm conversion associated with proton uptake has been long known as the "P_R" $\rightarrow$ **F** step observed during oxidation of the fully reduced aa_3 oxidases by oxygen [2,63].

The physical nature of the intense 607-610 nm absorption band in "compounds **P**" has not been established. Recent findings of a very similar band in the "P_R" [64] and "P_M" [65] intermediates of ba_3 oxidase from *T. thermophilus*, where the absorption of the low-spin heme b is well separated from the α-band of heme a_3, confirm at least that the band indeed belongs to heme a_3, and not to the low-spin heme a. As noted in [66] the narrowness of the α-band of "**P**"-state at ~607 nm may indicate that this form of heme a_3 is diamagnetic due to an uniaxial distortion of the heme plane sufficient to lower the energy of the d_{xz}-orbital by the amount required to cause complete pairing of the four d-electrons of the ferryl heme iron.

Interestingly, the intense band at 610-615 nm is retained during the "P_R" $\rightarrow$ **F** transition in the ba_3 oxidase from *T. thermophilus* [64] despite that two protons are taken up by the ba_3 oxidase during this transition as in the case of the aa_3 oxidases [67]. That intermediate F_{II} of ba_3 oxidase may retain the ~610 nm absorption band of F_I is also implied by recent work [65].

Apparently, the 607-610 nm band in the ferryl-oxo Compounds I and II of COX is not a marker of either the redox state of the intermediates, or of the order of their appearance in the catalytic site (cf. the "reversed **F** $\rightarrow$ P_N" reaction in [6]). Rather,

the band reports deprotonated state of some group(s) in the binuclear site.

The nature of the protonatable group(s) controlling the $607 \rightarrow 580$ nm transition remains to be established. In case of Compound II (the "P_R" $\rightarrow$ **F** transition), protonation of $Tyr244_{bt}$ in Cu_B^{2+}-His-TyrO$^-$ was proposed in [63] but was not confirmed [24], and most workers assign the "P_R" $\rightarrow$ **F** transition to protonation of Cu_B^{2+}-bound hydroxide to water [2,4,68]. It is noted that Cu_B coordination sphere may be viewed as a resonance structure H_2O-Cu_B-His-Tyr-O$^-$ $\leftrightarrow$ $^-$HO-Cu_B-His-Tyr-OH [14], and rapid equilibration of proton deficiency between the OH group of Tyr and Cu_B-bound water may depend on the enzyme species and specific conditions of the experiments.

Transition of Compound I from the 607 to the ~580 nm form is associated, as in the "P_R" $\rightarrow$ **F** step, with uptake of 1 proton by a group with pK > 9 [60]. Behaviour of the group is non-trivial. It can be rapidly protonated via the K-channel at the stage of Compound I formation during reaction of H_2O_2 with the oxidized COX [61]. However, after Compound I has been formed at pH >8, acidification results in but very slow $607 \rightarrow 580$ nm conversion ($k_v \sim0.03$ s^{-1} at pH 6.5 [60,61]) by virtue of proton leak through some unspecific pathway(s), as the rate it not affected by mutations in the proton channels [61]. At the same time, even very long preincubation of the oxidized enzyme with the blocked K-channel at acidic pH, by far sufficient to protonate the group via the unspecific leaks, does not prevent formation of the 607 nm intermediate upon addition of H_2O_2. Thus the protonatable group in question is likely to appear in the bincuclear site only after initiation of reaction with H_2O_2.

As proposed in [61], the ionizable group responsible for the $607 \rightarrow 580$ nm transition could be a water molecule inside the BNC reaction cavity formed upon scission of the O–O bond in the ferric-dihydroperoxy complex of heme a_3 (P_0 in Fig. 1) and connected protonically via $Tyr288_{rs}$ ($Tyr244_{bt}$) with the K-proton channel that is open at the stage of the O–O bond cleavage, but closes after formation of Compound I so that protonic connection of the BNC cavity with bulk water becomes blocked. This proposal is nicely supported by recent crystal structure analysis [21,43]: the authors deduce a structure for Compound I with a water molecule bridging the oxoferryl oxygen atom at the heme a_3 iron and the oxygen atom of $Tyr244_{bt}$. In this structure, additional hydrogen bonding of $Y244_{bt}$ oxygen to the OH group of the hydroxyethyl-farnesyl substituent of heme a_3 blocks protonic connection of the BNC cavity with the K-channel [9,21,43] in agreement with the "K-gate" model [22,55].

The protonation-dependent $607 \rightarrow 580$ nm transition of the ferryl-oxo intermediates of COX proved irreversible, i.e. nobody has been able so far to obtain the 607 nm form from the 580 nm state by raising pH, which was assigned to high pK of the group [60]. However, very recently, partial conversion of F_{II}-580 complex of COX to the 610 nm form by NH_3 or organic amines was demonstrated, the reaction being fully reversible [6]. The effect might be associated with binding of a strong base (:NH_3) to Cu_B^{2+}.

4. Membrane potential generation coupled to single-electron transfer steps in the catalytic cycle

Steady state turnover of the A-class cytochrome oxidases is coupled to translocations of 4 protons and 8 electric charges across the membrane per O_2 molecule reduced (Eq. (1)). In order to understand the overall energy-transduction mechanism, it is important to resolve charge translocation steps associated with single-electron interconversions between the adjacent intermediates in the cycle. Our studies have been mainly focused on the peroxidase part of the reaction. The peroxidase half of the cycle running via reaction of the added H_2O_2 with ferric heme a_3 in the oxidized COX

Table 1
Charge translocation coupled to transfer of the third and fourth electrons in the catalytic cycle of cytochrome oxidase from bovine mitochondria and *R. sphaeroides*.

The enzyme	Catalytic step	Characteristics of the electrogenic phases			$A_1/$ A_2	Refs.
		KCN-insensitive part (reduction of heme a) Rapid phase τ, α, q	KCN-inhibited part (reoxidation of heme a)			
			Intermediate phase τ, α, q	Slow phase τ, α, q		
Cytochrome oxidase from bovine heart mitochondria	Third electron ($F_I \rightarrow F_{II}$)	45 µs, 21%, 0.42	0.3 ms, 36%, 0.72	1.3 ms, 43%, 0.86	0.84	[40,80]
	Fourth electron ($F_{II} \rightarrow O$)	45 µs, 20%, 0.4	1.2 ms, 37%, 0.74	4.5 ms, 43%, 0.86	0.86	[75,103]
Cytochrome oxidase from *R. sphaeroides*	Third electron ($F_I \rightarrow F_{III}$)	13 µs, 28%, 0.56	0.18 ms, 50%, 1.0	0.85 ms, 22%, 0.44	2.3	[80]
	Fourth electron ($F_{II} \rightarrow O$)	15 µs, 29%, 0.58 10 µs, 17%, 0.34 (0.38)	40 µs, 12%, 0.24 (0.27)	0.4 ms, 33%, 0.66 (0.74)	1.6 ms, 38%, 0.76 (0.85)	0.87	[13,16,76]

For each partial step, the table gives time constant (τ), relative magnitude of the electrogenic phase in % of the overall response (α), and electrogenicity in unit charges translocated across the membrane (q). Electrogenicity of the phases (q) is estimated assuming that 2 unit charges are translocated across the membrane in each of the $F_I \rightarrow F_{II}$ and $F_{II} \rightarrow O$ transitions [4,82]. A_1/A_2, the magnitude ratio of the electrogenic protonic phases 1 and 2. Contributions of the protonic phases 1 and 2 have been recalculated from the original data [13,40,75,76] taking into account serial sequence of the kinetic steps [80,108]. In case of the $F_{II} \rightarrow O$ transition in the bacterial oxidase, the rapid phase was found to include two components (see the text and ref. [16]); characteristics of the two components of the rapid phase (10 µs $Cu_A \rightarrow$ heme *a* ET and ∼40 µs proton transfer step) are indicated in the lower part of the box. As discussed in [74] and depicted provisionally in Fig. 2B, the additional ∼40 µs protonic component of the rapid phase might originate in release of an extra proton pre-loaded to the PLS in Compound F_{II} by H_2O_2 upon its binding to heme iron; in such a case, the overall number of charges translocated in the $F_{II} \rightarrow O$ transition could be higher than 2 (∼2.24). The numbers in brackets in the bottom raw of the table give the q (electrogenicity) values re-calculated for such a case. Notably, the recalculated q values become very close to those observed for the $F_{II} \rightarrow O$ transition in the bovine COX.

and formation of Compounds I and II (blue contour in Fig. 1) can be resolved as a partial catalytic reaction [69–71] coupled to generation of membrane potential and proton pumping [70,72]. The peroxidase phase includes two single-electron transitions, $F_I \rightarrow F_{II}$ and $F_{II} \rightarrow O$, each coupled to proton pumping. Time-resolved electrometric studies of charge translocation linked to each of these transitions have been carried out with the mitochondrial and bacterial oxidases using single-electron photoreduction technique (reviewed, [1,73,74]).

Some of the results are summarized in Table 1. A generic pattern of $\Delta\psi$ generation coupled to the $F_I \rightarrow F_{II}$ and $F_{II} \rightarrow O$ transitions is shared by the mitochondrial and bacterial A-class oxidases and is characterized by 3 major phases of charge translocation. A *rapid* (microsecond) electrogenic phase associated with the KCN-insensitive reduction of heme *a* is mainly due to vectorial electron transfer from Cu_A to heme *a* (but see below); it is followed by two charge translocation phases of about equal magnitude associated with reoxidation of heme *a* by heme a_3 denoted as the *intermediate* and *slow* electrogenic phases [75] or the electrogenic protonic phases 1 and 2, respectively [76].

There are two points to be noted. First, the pattern of charge translocation coupled to the $F_I \rightarrow F_{II}$ ("P_M" $\rightarrow$ F) step, i.e. transfer of the 3rd e^- in the catalytic cycle of either mitochondrial or bacterial oxidase is very different from the electric response associated with the "P_R" $\rightarrow$ F transition resolved during the oxidation of the fully reduced enzyme by O_2 in the flow-flash experiments [77,78] (see [74] for detailed comparison). Second and more important, despite the common generic pattern, the electrogenic responses of the mitochondrial and bacterial oxidases differ in several important details.

In bovine oxidase, the patterns of charge translocation coupled to transfer of the 3rd and 4th electrons are very similar except that the protonic phases associated with oxidation of heme *a* are 2-3-fold faster for the $F_I \rightarrow F_{II}$ transition (Table 1). In particular, the overall number of charges translocated across the membrane during the $F_I \rightarrow F_{II}$ and $F_{II} \rightarrow O$ steps transitions was shown to be the same [40]. Translocation of ∼0.4 elementary charges in the rapid phase is within the range of values calculated theoretically for the electrogenicity of the $Cu_A \rightarrow$ heme *a* vectorial electron transfer in [79], although the value might be slightly overestimated in case

of incomplete formation of the ferryl-oxo state of heme a_3 prior to electron photoinjection. Importantly, the same [protonic phase 1]/ [protonic phase 2] magnitude ratio, $A_1/A_2 = 0.84 – 0.86$, is observed for the $F_I \rightarrow F_{II}$ and $F_{II} \rightarrow O$ transitions, and in the both transitions it is the electrogenic protonic phase 1 that matches ET from heme *a* to heme a_3, whereas the major part of the protonic phase 2 takes place after completion of heme oxidoreduction [12,74,80,81]. Thus, the mechanisms of charge translocation coupled to transfer of the 3rd and 4th electrons in the mitochondrial oxidase are likely to be much the same.

The bacterial enzyme reveals a number of distinctive features, apart from the 3-4-fold faster rates for each phase which correlates with the 3-4-fold faster turnover of the bacterial oxidase. First, contribution of the KCN-insensitive "rapid" electrogenic phase is significantly higher (∼30% of the overall response). The same high contribution of the rapid phase has been observed for the $F_{II} \rightarrow O$ transition in the bacterial aa_3 COX from *P. denitrificans* [17]. As found in [16], the rapid phase in *R. sphaeroides* oxidase is heterogenous and may include a minor contribution from a ∼40 µs internal proton transfer step in addition to the 10 µs vectorial ET from Cu_A to heme *a* (Table 1, the bottom raw). Second, in the $F_I \rightarrow F_{II}$ transition of bacterial COX, the number of charges translocated in the protonic phase 1 is 2.3-fold higher than in the protonic phase 2, as observed both for the *R. sphaeroides* (Table 1, [80]) and *P.denitrificans* oxidases [82,74], whereas the corresponding ratio for the $F_{II} \rightarrow O$ step is ∼0.87, close to that in the mitochondrial oxidase (Table 1, [74]). Therefore, the protonmotive mechanisms associated with transfer of the 3rd and 4th electrons in the bacterial oxidases can hardly be the same. Third, in COX from *R. sphaeroides*, the two protonic electrogenic phases in the $F_{II} \rightarrow O$ transition match closely the two phases of heme *a* reoxidation by ferryl-oxo complex of heme a_3 ([16,76]) whereas in the mitochondrial oxidase, heme *a* reoxidation is coupled almost exclusively to the electrogenic protonic phase 1 [12,74,80,81].

These and other differences (cf. [74]) suggest that the attempts to invoke a uniform protonmotive mechanism for all the single-electron steps in the catalytic cycle of COX, as well as for the same step in the different A-class oxidases (e.g. [1,82–84]), may be a deceptive simplification. Each single-electron step in the catalytic cycle in each enzyme species may need to be investigated

separately (cf. [85]). That the mechanism of proton translocation by mammalian COX is different from that in the bacterial A-class oxidases has been argued persistently by Yoshikawa and co-workers [26,44,86].

5. Partial electrogenic steps within the single-electron transitions of COX

One of the lessons from Antonio Xavier as he published his papers on cytochrome oxidase [87,88] was that the mechanism of coupling between electron and proton transfer in cytochrome oxidase should not be reduced to a paradigm of electrostatic effects: e.g., to an assumption that reduction of a redox center is coupled electrostatically to proton binding by some nearby ionizable group, and that oxidation of the center leads to release of the proton. Perturbation induced by addition of an electron to a redox center can be transmitted through the protein via a specific chain of complex mechanochemical interactions leading at the end of the chain to perturbation of proton affinity of some group in *either* direction. Addition of an electron, say, to heme *a* may be coupled to proton uptake, or internal proton displacement, or even to proton release as proposed for instance in [44,86–88]. This view may be related to the concept of mechanically programmed *molecular machine* developed in Moscow by Blumenfeld [89] (and cf. a model of redox-induced conformationally coupled multiple pK changes in COX held to by Bari group [90]). A fascinating picture of articulate intra-protein group movements/adjustments coupled to the reduction of heme *a* via electrostatic and mechanical interactions that enable proton disclocation from E242$_{bt}$ at the bottom of the D-channel via Δpropionate of heme a_3 and to the "Proton Loading Site" (PLS, cluster of interacting protonatable groups "above the hemes") is revealed by theoretical calculations and molecular dynamics simulations (reorientation of E242$_{bt}$ [91,92], formation and polarization of the water chains leading from E242 to ΔPro of heme a_3 [93,94], loosening of hydrogen bonding of ΔPro with the arginines [25] and swinging of ΔPro to reach the water chain leading from E242 [95], etc.).

A generic scheme of partial charge translocation steps coupled to transfer of a single electron through cytochrome oxidase was formulated early [83,96]. The model proposed, long before the crystal structure of COX was solved [97,98], spatial arrangement of hemes *a* and a_3 along rather than across the membrane, and predicted involvement of protonic channels in charge translocation by the enzyme (Fig. 2A).

The basic partial steps of the protonmotive mechanism denoted in Fig. 2A by arrows were rightly guessed, as confirmed by subsequent experimental work and theoretical modeling (reviewed, [1,3,4,74,79,99]). However, the original sequence of the steps (it will correspond to $1 \to 3 \to 2 \to 4 \to 6 \to 5$ in Fig. 2A) was based on a simplistic paradigm of electrostatic interactions criticized by Antonio Xavier [87,88] and had to be modified as shown in the figure. Thus, it was proposed originally that reduction of heme *a* (step 1) is electrostatically coupled to uptake of the pumped proton from the *N*-phase via the input proton channel (step 3). The proton is then transferred from the bottom of the input proton well to the bottom of the exit proton well – i.e., from E286 to the Proton Loading Site (PLS) in modern terminology (step 2 in the scheme), – which gates ET from heme *a* to the binuclear site (step 4). Upon ET from heme *a* to heme a_3, the proton from PLS is released to the *P*-phase (step 6), and a chemical proton is taken up to neutralize the negative charge brought by electron to the binuclear site (step 5). The currently assumed picture of the events includes essentially the same basic steps as Fig. 2A (e.g. [84,100]) but is more elaborate.

A plausible electrogenic mechanism specifically relevant to the **F$_{II}$ → O** transition in COX and based essentially on the time-resolved
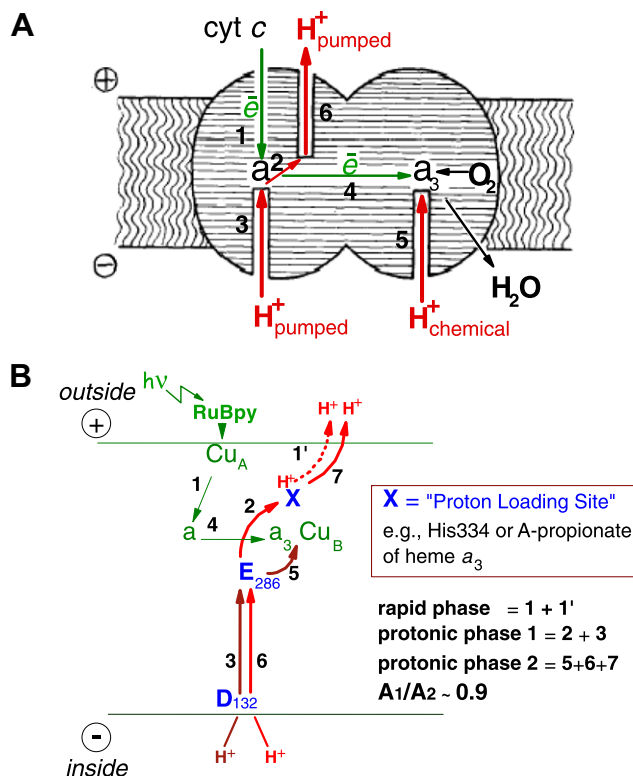

Fig. 2. Protonmotive mechanism coupled to transfer of a single electron through cytochrome oxidase. (A) A generic scheme is given essentially as it was presented in refs. [83,96]. The numbers indicate the currently presumed sequence of the partial steps. The order of the steps originally proposed in [83,96] was $1 \to 3 \to 2 \to 4 \to 6 \to 5$ (see section 5 of the text). (B). A specific version of the generic scheme as adapted for the **F$_{II}$ → O** transition. **A$_1$/A$_2$**, the magnitude ratio of the electrogenic protonic phases 1 and 2 (cf. Table 1). The scheme corresponds primarily to *R. sphaeroides* COX for which most of the data have been obtained. In the **F$_{II}$ → O** transition of *R. sphaeroides* oxidase, the two protons are presumed to be taken up from the *N*-phase via the same D-proton channel, and the electrogenic protonic phases 1 and 2 are dominated by the two sequential reprotonations of E286 at the intramembrane end of the D-channel from the *N*-phase (steps 3 and 6) after E286 donates its proton first to the PLS (step 2) and then to the binuclear site (step 5); the latter partial step has been resolved experimentally in the non-pumping mutant N139L, in which reprotonation of E286 from the *N*-phase is blocked [16]. The experimentally observed **A$_1$/A$_2$** ratio of ~0.9 agrees with the "electric" location of the groups considered within the protein dielectric as calculated in [79]. Proton transfer step 1′ coupled to electron transfer step 1 has been included provisionally in the scheme as one of the possible explanations of the heterogeneity of the rapid electrogenic phase in the **F$_{II}$ → O** transition of the bacterial oxidase [16] (see the text for discussion). The partial steps of the "chemical" and "pumped" proton transfer are intertwined intricately in the two protonic phases. On the one hand, H$^+$ transfer from E286 to PLS (step 2) followed by reprotonation of E286 (step 3) may be viewed as delivery of the pumped proton from the *N*-phase to PLS; accordingly, subsequent transfer of proton from E286 to BNC (step 5) followed by the second reprotonation of E286 from the *N*-phase (step 6) would be regarded as uptake of the "chemical" proton by BNC from the *N*-phase (e.g., see Fig. 5 in [74]). On the other hand, if we take into consideration *destination* of the protons, then the proton taken up by E286 at step 3 is destined to protonate BNC (via step 5), and, hence, may be considered as "chemical", whereas the H$^+$ taken up by E286 at step 6 is destined to be pumped out during the transfer of the next electron in the cycle; the destination-based attribution of the protons as "chemical" (dark red) or "pumped" (bright red) is indicated in the scheme by color coding. I would acknowledge that this peculiar ambiguity in referring the protons taken up from the *N*-phase as "pumped" or "chemical" was pointed out by Dr. N. Azarkina in this laboratory, during discussion of the problem at a seminar.

electrometric and absorption measurements [13,16,40,75,76,80,81,101–103] correlated with the available crystal structure of the enzyme and theoretical modeling [55,79,93,94,104] is shown in Fig. 2B. A similar general scheme though not assigned to any specific single-electron step was considered in [84]. Unfortunately, important complementing information from the time-resolved

proton uptake/release measurements, available in the case of the flow-flash experiment studies on the oxidation of the fully reduced oxidase by oxygen (e.g. [105] and see the reviews [3,15]), is virtually missing for the single-electron reduction experiments [103].

In variance with the original scheme [83,96], the proton to be pumped outside is sitting at the bottom of the input D-channel (protonated E286$_{rs}$) prior to reduction of heme *a*. Reduction of heme *a* by Cu$_A$ gives rise to the rapid electrogenic phase (step 1) which is coupled energetically to *deprotonation* of E286 and relocation of the pumped H$^+$ to the PLS (step 2), which is followed by immediate reprotonation of E286 from the *N*-phase (step 3) and gates oxidation of heme *a* by the ferryl-oxo complex of heme *a*$_3$ (non-electrogenic step 4). As a matter of fact, the exact order of the steps 2,3,4 has not been determined (e.g., it could be 4,2,3 [76,84] or even 2,4,3). The proton transfer steps 2 and 3 merge kinetically giving rise to the experimentally observed electrogenic protonic phase 1 coupled kinetically to partial (in *R. sphaeroides*) or almost complete (in bovine oxidase) ET from heme *a* to the binuclear site. Similarly, subsequent release of the pumped proton from the PLS to the *P*-phase (step 7), and protonation of the reduced binuclear site from the *N*-phase induced by reduction of the ferryl-oxo complex of heme *a*$_3$ (steps 5,6) appear to be synchronous under most conditions (cf. ref. [105]), and show up as a single concerted process; so, the vectorial proton transfer steps 5,6 and 7 merge into a single electrogenic protonic phase 2. It is currently thought that as first proposed by Rich [106], uptake of the "chemical" proton from the *N*-phase precedes proton extrusion from the PLS to the *P*-side and even provides a driving force for it of ca. 0.2 eV [107]. Hence, the order of the steps 5,6,7 in Fig. 2B has been chosen to conform to this proposal.

The scheme in Fig. 2B corresponds primarily to the F$_{II}$ → O transition in COX from *R. sphaeroides*. That it may also apply to the F$_{II}$ → O and F$_I$ → F$_{II}$ steps in the mitochondrial oxidase may be assumed by analogy taking into account general similarity of the electrogenic responses (except for step 1', see below). In particular, the experimentally observed ratio of the two KCN-sensitive electrogenic protonic phases in the F$_{II}$ → O transition of the *R. sphaeroides* COX, A$_1$/A$_2$ = 0.87, is very close to the A$_1$/A$_2$ ratio values found for the F$_{II}$ → O and F$_I$ → F$_{II}$ steps in the bovine oxidase, which favors the same attribution of the protonic phases. However, the same specific usage of the proton channels in the bacterial and mammalian oxidases has not yet been confirmed experimentally and remains be verified (cf. [26]). Notably, the scheme in Fig. 2B cannot accommodate the A$_1$/A$_2$ value of 2.3 observed for the F$_I$ → F$_{II}$ transition in the bacterial oxidases from *R. sphaeroides* and *P. denitrificans* (Table 1, [74,80,82]). Attribution of the protonic phases 1 and 2 has to be very different in this case, so the specific mechanisms of proton pumping coupled to transfer of the 3rd and 4th electrons, while similar in the bovine oxidase, appear to be different in the bacterial oxidases.

Step 1' linked to step 1 has been included provisionally in Fig. 2B to illustrate one of the several possible interpretations of the KCN-insensitive ~40 μs protonic component of the *rapid* electrogenic phase in the bacterial oxidases (Table 1, [16,74]). This provisional explanation is based on the crystal structure analysis and theoretical modeling in [55,104] predicting that oxidation of Cu$_A$ during the Cu$_A$ → heme *a* ET may be coupled to release of a proton from the PLS to the *P*-phase, given the PLS is protonated prior to initiation of ET. The protonation state of the PLS in different intermediates of the catalytic cycle is not known but according to the electrostatic calculations [84], the [Fe^{4+} = O^{2-}/Cu^{2+}–OH$^-$] state of the BNC in the F$_{II}$ intermediate generated by the reaction of the oxidized bacterial COX with H$_2$O$_2$ would be consistent with the protonated state of Nδ1 in His334$_{rs}$ (H291$_{bt}$). It can be remarked that H$_2$O$_2$ is likely to bind to heme iron as OOH$^-$, placing its second proton to some near by protein group. Variation of the initial pro-

tonation state of the PLS among the single-electron transitions in the oxidases from different organisms, as well as among the 4 different single-electron transitions in the same enzyme, could explain variability of the magnitude of the rapid electrogenic phase in the single-electron photoreduction experiments, e.g. the difference between the mammalian and bacterial oxidases in the F$_{II}$ → O and F$_I$ → F$_{II}$ steps (Table 1).

Acknowledgements

References

[1] Belevich, I. and Verkhovsky, M.I. (2008) Molecular mechanism of proton translocation by cytochrome *c* oxidase. Antioxid. Redox Signaling 10, 1–29.

[2] Hosler, J.P., Ferguson-Miller, S. and Mills, D.A. (2006) Energy transduction:proton transfer through the respiratory complexes. Annu. Rev. Biochem. 75, 165–187.

[3] Brzezinski, P. and Gennis, R.B. (2008) Cytochrome *c* oxidase: exciting progress and remaining mysteries. J. Bioenerg. Biomembr. 40, 521–531.

[4] Kaila, V.R.I., Verkhovsky, M.I. and Wikstrom, M. (2010) Proton-coupled electron transfer in cytochrome oxidase. Chem. Rev. 110, 7062–7081.

[5] Chance, B., Saronio, C. and Leigh, J.S. (1975) Functional intermediates in reaction of cytochrome oxidase with oxygen. Proc. Natl. Acad. Sci. USA 72, 1635–1640.

[6] von der Hocht, I., van Wonderen, J.H., Hilbers, F., Angerera, H., MacMillan, F. and Michel, H. (2011) Interconversions of P and F intermediates of cytochrome *c* oxidase from *Paracoccus denitrificans*. Proc. Natl. Acad. Sci. USA 108, 3964–3969.

[7] Sono, M., Roach, M.P., Coulter, E.D. and Dawson, J.H. (1996) Heme-containing oxygenases. Chem. Rev. 96, 2841–2887.

[8] Blomberg, L.M., Blomberg, M.R.A. and Siegbahn, P.E.M. (2005) A theoretical study on the binding of O$_2$, NO and CO to heme proteins. J. Inorg. Biochem. 99, 949–958.

[9] Yoshioka, Y. and Mitani, M. (2010) B3LYP study on reduction mechanisms from O$_2$ to H$_2$ O at the catalytic sites of fully reduced and mixed-valence bovine cytochrome *c* oxidases. Bioinorg. Chem. Appl. 182804.

[10] Kaila, V.R., Oksanen, E., Goldman, A., Bloch, D.A., Verkhovsky, M.I., Sundholm, D. and Wikstrom, M. (2011) A combined quantum chemical and crystallographic study on the oxidized binuclear center of cytochrome *c* oxidase. Biochim. Biophys. Acta 1807, 769–778.

[11] Wikstrom, M., Krab, K. and Saraste, M. (1981) Cytochrome oxidase – a synthesis, Academic Press, New York.

[12] Konstantinov, A. (1998) Cytochrome *c* oxidase as a proton-pumping peroxidase: Reaction cycle and electrogenic mechanism. J. Bioenerg. Biomembr. 30, 121–130.

[13] Konstantinov, A.A., Siletsky, S., Mitchell, D., Kaulen, A. and Gennis, R.B. (1997) The roles of the two proton input channels in cytochrome *c* oxidase from Rhodobacter sphaeroides probed by the effects of site-directed mutations on time resolved electrogenic intraprotein proton transfer. Proc. Natl. Acad. Sci. USA 94, 9085–9090.

[14] Einarsdottir, O. and Szundi, I. (2004) Time-resolved optical absorption studies of cytochrome oxidase dynamics. Biochim. Biophys. Acta 1655, 263–273.

[15] Brzezinski, P. and Larsson, G. (2003) Redox-driven proton pumping by heme-copper oxidases. Biochim. Biophys. Acta 1605, 1–13.

[16] Siletsky, S.A., Zhu, J., Gennis, R.B. and Konstantinov, A.A. (2010) Partial steps of charge translocation in the nonpumping N139L mutant of *Rhodobacter sphaeroides* cytochrome *c* oxidase with a blocked D-channel. Biochemistry 49, 3060–3073.

[17] Ruitenberg, M., Kannt, A., Bamberg, E., Fendler, K. and Michel, H. (2002) Reduction of cytochrome *c* oxidase by a second electron leads to proton translocation. Nature 417, 99–102.

[18] Blomberg, M.R.A., Siegbahn, P.E.M., Babcock, G.T. and Wikstrom, M. (2000) Modeling cytochrome oxidase: A quantum chemical study of the O–O bond cleavage mechanism. J. Am. Chem. Soc. 122, 12848–12858.

[19] Yoshioka, Y., Satoh, H. and Mitani, M. (2007) Theoretical study on electronic structures of FeOO, FeOOH, FeO(H$_2$O), and FeO in hemes: As intermediate models of dioxygen reduction in cytochrome *c* oxidase. J. Inorg. Biochem. 101, 1410–1427.

[20] Hlavica, P. (2004) Models and mechanisms of O–O bond activation by cytochrome P450. Eur. J. Biochem. 271, 4335–4360.

[21] Yoshikawa, S., Muramoto, K. and Shinzawa-Itoh, K. (2011) The O$_2$ reduction and proton pumping gate mechanism of bovine heart cytochrome *c* oxidase. Biochim. Biophys. Acta doi:10.1016/j.bbabio.2011.06.008.

[22] Qin, L., Liu, J., Mills, D.A., Proshlyakov, D.A., Hiser, C. and Ferguson-Miller, S. (2009) Redox dependent conformational changes in cytochrome *c* oxidase suggest a gating mechanism for proton uptake. Biochemistry 48, 5121–5130.

[23] Moody, A.J. (1996) "as prepared" forms of fully oxidised haem/Cu terminal oxidases. Biochim. Biophys. Acta 1276, 6–20.

[24] Gorbikova, E.A., Wikstrom, M. and Verkhovsky, M.I. (2008) The protonation state of the cross-linked tyrosine during the catalytic cycle of cytochrome c oxidase. J. Biol. Chem. 283, 34907–34912.

[25] Kaila, V.R., Sharma, V. and Wikstrom, M. (2011) The identity of the transient proton loading site of the proton-pumping mechanism of cytochrome c oxidase. Biochim. Biophys. Acta 1807, 80–84.

[26] Yoshikawa, S., Muramoto, K. and Shinzawa-Itoh, K. (2011) Proton-pumping mechanism of cytochrome c oxidase. Annu. Rev. Biophys. 40, 205–223.

[27] Koepke, J., Olkhova, E., Angerer, H., Muller, H., Peng, G. and Michel, H. (2009) High resolution crystal structure of *Paracoccus denitrificans* cytochrome c oxidase: New insights into the active site and the proton transfer pathways. Biochim. Biophys. Acta 1787, 635–645.

[28] Fabian, M., Skultety, L., Jancura, D. and Palmer, G. (2004) Implications of ligand binding studies for the catalytic mechanism of cytochrome c oxidase. Biochim. Biophys. Acta 1655, 298–305.

[29] Suga, M.Y.N., Muramoto, K., Shinzawa-Itoh, K., Maeda, T., Yamashita, E., Tsukihara, T. and Yoshikawa, S. (2011) Distinguishing between Cl- and O22- as the bridging element between Fe3+ and Cu2+ in resting-oxidized cytochrome c oxidase. Acta Crystallogr. D: Biol. Crystallogr. 67, 742.

[30] Pereira, M.M., Santana, M. and Teixeira, M. (2001) A novel scenario for the evolution of haem-copper oxygen reductases. Biochim. Biophys. Acta 1505, 185–208.

[31] Aoyama, H., Muramoto, K., Shinzawa-Itoh, K., Hirata, K., Yamashita, E., Tsukihara, T., Ogura, T. and Yoshikawa, S. (2009) A peroxide bridge between Fe and Cu ions in the O2 reduction site of fully oxidized cytochrome c oxidase could suppress the proton pump. Proc. Natl. Acad. Sci. USA 106, 2165–2169.

[32] Tiefenbrunn, T., Liu, W., Chen, Y., Katritch, V., Stout, C.D., Fee, J.A. and Cherezov, V. (2011) High resolution structure of the ba_3 cytochrome c oxidase from *Thermus thermophilus* in a lipidicenvironment. PLoS ONE 6, e22348.

[33] Sakaguchi, M., Shinzawa-Itoh, K., Yoshikawa, S. and Ogura, T. (2010) A resonance Raman band assignable to the O–O stretching mode in the resting oxidized state of bovine heart cytochrome c oxidase. J. Bioenerg. Biomembr. 42, 241–243.

[34] Han, S., Takahashi, S. and Rousseau, D.L. (2000) Time dependence of the catalytic intermediates in cytochrome c oxidase. J. Biol. Chem. 275, 1910–1919.

[35] Ogura, T., Hirota, S., Proshlyakov, D., Shinzawa-Itoh, K., Yoshikawa, S. and Kitagawa, T. (1996) Time-resolved resonance Raman evidence for tight coupling between electron transfer and proton pumping of cytochrome c oxidase upon the change from the Fev oxidation level to the Feiv oxidation level. J. Am. Chem. Soc. 118, 5443–5449.

[36] Bloch, D., Belevich, I., Jasaitis, A., Ribacka, C., Puustinen, A., Verkhovsky, M.I. and Wikstrom, M. (2004) The catalytic cycle of cytochrome c oxidase is not the sum of its two halves. Proc. Natl. Acad. Sci. USA 101, 529–533.

[37] Belevich, I., Bloch, D.A., Wikstrom, M. and Verkhovsky, M.I. (2007) Exploring the proton pump mechanism of cytochrome c oxidase in real time. Proc. Natl. Acad. Sci. USA 104, 2685–2690.

[38] Siletsky, S.A., Belevich, I., Wikstrom, M., Soulimane, T. and Verkhovsky, M.I. (2009) Time-resolved Oh- Eh transition of the aberrant ba3 oxidase from *Thermus thermophilus*. Biochim. Biophys. Acta 1787, 201–205.

[39] Siletsky, S.A., Belevich, I., Belevich, N.P., Soulimane, T. and Verkhovsky, M.I. (2011) Time-resolved single-turnover of caa_3 oxidase from *Thermus thermophilus*. Fifth electron of the fully reduced enzyme converts O_H into E_H state. Biochim. Biophys. Acta 1807, 1162–1169.

[40] Siletsky, S., Kaulen, A.D. and Konstantinov, A.A. (1999) Resolution of electrogenic steps coupled to conversion of cytochrome c oxidase from the peroxy to the ferryl-oxo state. Biochemistry 38, 4853–4861.

[41] Verkhovsky, M.I., Tuukkanen, A., Backgren, C., Puustinen, A. and Wikstrom, M. (2001) Charge translocation coupled to electron injection into oxidized cytochrome c oxidase from *Paracoccus denitrificans*. Biochemistry 40, 7077–7083.

[42] Jancura, D., Berka, V., Antalik, M., Bagelova, J., Gennis, R.B., Palmer, G. and Fabian, M. (2006) Spectral and kinetic equivalence of oxidized cytochrome c oxidase as isolated and "activated" by reoxidation. J. Biol. Chem. 281, 30319–30325.

[43] Muramoto, K., Ohta, K., Shinzawa-Itoh, K., Kanda, K., Taniguchi, M., Nabekura, H., Yamashita, E., Tsukihara, T. and Yoshikawa, S. (2010) Bovine cytochrome c oxidase structures enable O2 reduction with minimization of reactive oxygens and provide a proton-pumping gate. Proc. Natl. Acad. Sci. USA 107, 7740–7745.

[44] Yoshikawa, S., Shinzawa-Itoh, K., Nakashima, R., Yaono, R., Inoue, N., Yao, M., Fei, M.J., Libeu, C.P., Mizushima, T., Yamaguchi, H., Tomizaki, T. and Tsukihara, T. (1998) Redox-coupled crystal structural changes in bovine heart cytochrome c oxidase. Science 280, 1723–1729.

[45] Einarsdottir, O. (1995) Fast reactions of cytochrome oxidase. Biochim. Biophys. Acta 1229, 129–147.

[46] Koutsoupakis, K., Stavrakis, S., Pinakoulaki, E., Soulimane, T. and Varotsis, C. (2002) Observation of the equilibrium Cu_B-CO complex and functional implication of the transient heme a_3-CO from *Thermus thermophilus*. J. Biol. Chem. 277, 32860–32866.

[47] Blomberg, M.R.A., Siegbahn, P.E.M. and Wikstrom, M.K.F. (2003) Metal-bridging mechanism for O–O bond cleavage in cytochrome c oxidase. Inorg. Chem. 42, 5231–5243.

[48] Halime, Z., Kotani, H., Li, Y., Fukuzumi, S. and Karlin, K.D. (2011) Homogeneous catalytic O2 reduction to water by a cytochrome c oxidase model with trapping of intermediates and mechanistic insights. Proc. Natl. Acad. Sci. USA 108, 13990–13994.

[49] Proshlyakov, D.A. (2004) UV optical absorption by protein radicals in cytochrome c oxidase. Biochim. Biophys. Acta 1655, 282–289.

[50] Wiertz, F.G.M., Richter, O.-M.H., Cherepanov, A.V., MacMillan, F., Ludwig, B. and de Vries, S. (2004) An oxo-ferryl tryptophan radical catalytic intermediate in the reaction of cytochrome c and quinol oxidases trapped by microsecond freeze-hyperquenching (MNQ). FEBS Lett. 575, 127–130.

[51] Siegbahn, P. and Blomberg, M.R.A. (2004) Important roles of tyrosines in photosystem ii and cytochrome oxidase. Biochim. Biophys. Acta 1655, 45–50.

[52] Wiertz, F.G.M., Richter, O.-M.H., Ludwig, B. and de Vries, S. (2007) Kinetic resolution of a tryptophan-radical intermediate in the reaction cycle of *Paracoccus denitrificans* cytochrome c oxidase. J. Biol. Chem. 282, 31580–31591.

[53] MacMillan, F., Budiman, K., Angerer, H. and Michel, H. (2006) The role of triptophan 272 in the *Paracoccus denitrificans* cytochrome c oxidase. FEBS Lett. 580, 1345–1349.

[54] de Vries, S. (2008) The role of the conserved tryptophan272 of the *Paracoccus denitrificans* cytochrome c oxidase in proton pumping. Biochim. Biophys. Acta 1777, 925–928.

[55] Sharpe, M.A. and Ferguson-Miller, S. (2008) A chemically explicit model for the mechanism of proton pumping in heme-copper oxidases. J. Bioenerg. Biomembr. 40, 541–549.

[56] Budiman, K., Kannt, A., Lyubenova, S., Richter, O.-M.H., Ludwig, B., Michel, H. and MacMillan, F. (2004) Tyrosin 167: The origin of the radical species observed in the reaction of cytochrome c oxidase with hydrogen peroxide in *Paracoccus denitrificans*. Biochemistry 43, 11709–11716.

[57] Svistunenko, D.A., Wilson, M.T. and Cooper, C.E. (2004) Tryptophan or tyrosine? On the nature of the amino acid radical formed following hydrogen peroxide treatment of cytochrome c oxidase. Biochim. Biophys. Acta 1655, 372–380.

[58] Yu, M.A., Egawa, T., Shinzawa-Itoh, K., Yoshikawa, S., Yeh, S.-R., Rousseau, D.L. and Gerfen, G.J. (2011) Radical formation in cytochrome c oxidase. Biochim. Biophys. Acta doi:10.1016/j.bbabio.2011.06.012.

[59] Vygodina, T. and Konstantinov, A. (1989) Effect of pH on the spectrum of cytochrome c oxidase hydrogen peroxide complex. Biochim. Biophys. Acta 973, 390–398.

[60] Fabian, M. and Palmer, G. (2001) Proton involvement in the transition from the "peroxy" to the ferryl intermediate of cytochrome c oxidase. Biochemistry 40, 1867–1874.

[61] Pecoraro, C., Gennis, R.B., Vygodina, T.V. and Konstantinov, A.A. (2001) Role of the K-channel in the pH-dependence of the reaction of cytochrome c oxidase with hydrogen peroxide. Biochemistry 40, 9695–9708.

[62] Rich, P.R., Rigby, S.E. and Heathcote, P. (2002) Radicals associated with the catalytic intermediates of bovine cytochrome c oxidase. Biochim. Biophys. Acta 1554, 137–146.

[63] Belevich, I., Verkhovsky, M.I. and Wikstrom, M. (2006) Proton-coupled electron transfer drives the proton pump of cytochrome c oxidase. Nature 440, 829–832.

[64] Siletsky, S.A., Belevich, I., Jasaitis, A., Konstantinov, A.A., Wikstrom, M., Soulimane, T. and Verkhovsky, M.I. (2007) Time-resolved single-turnover of ba_3 oxidase from *Thermus thermophilus*. Biochim. Biophys. Acta 1767, 1383–1392.

[65] Koutsoupakis, C., Kolaj-Robin, O., Soulimane, T. and Varotsis, C. (2011) Probing the protonation/deprotonation of tyrosine residues in cytochrome ba 3 oxidase from *Thermus thermophilus* by time-resolved step-scan FTIR spectroscopy. J. Biol. Chem. 286, 30600–30605.

[66] Fabian, M. and Palmer, G. (1999) Redox state of peroxy and ferryl intermediates in cytochrome c oxidase catalysis. Biochemistry 38, 6270–6275.

[67] von Ballmoos, C., Gennis, R.B., Adelroth, P. and Brzezinski, P. (2011) Kinetic design of the respiratory oxidases. Proc. Natl. Acad. Sci. USA 108, 11057–11062.

[68] Branden, G., Gennis, R.B. and Brzezinski, P. (2006) Transmembrane proton translocation by cytochrome c oxidase. Biochim. Biophys. Acta 1757, 1052–1063.

[69] Konstantinov, A.A., Vygodina, T.V., Capitanio, N. and Papa, S. (1998) Ferrocyanide peroxidase activity of cytochrome c oxidase. Biochim. Biophys. Acta 1363, 11–23.

[70] Vygodina, T.V., Pecoraro, C., Mitchell, D., Gennis, R. and Konstantinov, A.A. (1998) The mechanism of inhibition of electron transfer by amino acid replacement K362M in a proton channel of *Rhodobacter sphaeroides* cytochrome c oxidase. Biochemistry 37, 3053–3061.

[71] Vygodina, T.V. and Konstantinov, A.A. (2007) Peroxidase activity of mitochondrial cytochrome c oxidase. Biochemistry (Moscow) 72, 1300–1310.

[72] Vygodina, T.V., Capitanio, N., Papa, S. and Konstantinov, A.A. (1997) Proton pumping by cytochrome c oxidase is coupled to peroxidase half of its catalytic cycle. FEBS Lett. 412, 405–409.

[73] Geren, L., Durham, B. and Millett, F. (2009) Use of ruthenium photoreduction techniques to study electron transfer in cytochrome oxidase. Methods Enzymol. 456, 507–520.

[74] Siletsky, S. and Konstantinov, A.A. (2011) Cytochrome c oxidase: Charge translocation coupled to single-electron partial steps of the catalytic cycle. Biochim. Biophys. Acta, doi:10.1016/j.bbabio.2011.08.003.

[75] Zaslavsky, D., Kaulen, A., Smirnova, I.A., Vygodina, T.V. and Konstantinov, A.A. (1993) Flash-induced membrane potential generation by cytochrome *c* oxidase. FEBS Lett. 336, 389–393.

[76] Siletsky, S.A., Pawate, A.S., Weiss, K., Gennis, R.B. and Konstantinov, A.A. (2004) Transmembrane charge separation during the ferryl-oxo → oxidized transition in a non-pumping mutant of cytochrome c oxidase. J. Biol. Chem. 279, 52558–52565.

[77] Jasaitis, A., Verkhovsky, M.I., Morgan, J.E., Verkhovskaya, M.L. and Wikstrom, M. (1999) Assignment and charge translocation stoichiometries of the electrogenic phases in the reaction of cytochrome *c* with dioxygen. Biochemistry 38, 2697–2706.

[78] Lepp, H. and Brzezinski, P. (2009) Internal charge transfer in cytochrome c oxidase at a limited proton supply: Proton pumping ceases at high pH. Biochim. Biophys. Acta 1790, 552–557.

[79] Sugitani, R., Medvedev, E.S. and Stuchebrukhov, A.A. (2008) Theoretical and computational analysis of the membrane potential generated by cytochrome c oxidase upon single electron injection into the enzyme. Biochim. Biophys. Acta 1777, 1129–1139.

[80] Siletsky, S.A., Han, D., Brand, S., Morgan, J.E., Fabian, M., Geren, L., Millett, F., Durham, B., Konstantinov, A.A. and Gennis, R.B. (2006) Single-electron photoreduction of the P$_M$ intermediate of cytochrome *c* oxidase. Biochim. Biophys. Acta 1757, 1122–1132.

[81] Siletsky, S.A. (1998) Studies of electrogenic transfer of protons in cytochrome oxidase. Ph.D. thesis, Moscow State University, Moscow, pp. 1–108.

[82] Verkhovsky, M.I., Belevich, I., Bloch, D.A. and Wikstrom, M. (2006) Elementary steps of proton translocation in the catalytic cycle of cytochrome oxidase. Biochim. Biophys. Acta 1757, 401–407.

[83] Artzatbanov, V.Y., Konstantinov, A.A. and Skulachev, V.P. (1978) Involvement of intramitochondrial protons in redox reactions of cytochrome *a*. FEBS Lett. 87, 180–185.

[84] Popovic, D.M. and Stuchebryukhov, A.A. (2004) Proton pumping mechanism and catalytic cycle of cytochrome c oxidase: Coulomb pump model with kinetic gating. FEBS Lett. 566, 126–130.

[85] Michel, H. (1999) Cytochrome c oxidase: Catalytic cycle and mechanism of proton pumping – a discussion. Biochemistry 38, 15129–15140.

[86] Yoshikawa, S., Shinzawa-Itoh, K. and Tsukihara, T. (2000) X-ray structure and the reaction mechanism of bovine heart cytochrome *c* oxidase. J. Inorg. Biochem. 82, 1–7.

[87] Xavier, A.V. (2002) A mechano-chemical model for energy trunsduction in cytochrome *c* oxidase: The work of a Maxwell's God. FEBS Lett. 532, 261–266.

[88] Xavier, A.V. (2004) Thermodynamic and choreographic constraints for energy transduction by cytochrome *c* oxidase. Biochim. Biophys. Acta 1658, 23–30.

[89] Blumenfeld, L.A. (1977) Problems of Biological Physics, Nauka press, Moscow.

[90] Papa, S., Capitanio, N., Capitanio, G. and Palese, L. (2004) Protonmotive cooperativity in cytochrome *c* oxidase. Biochim. Biophys. Acta 1658, 95–105.

[91] Popovic, D.M. and Stuchebrukhov, A.A. (2006) Two conformational states of Glu242 and pK$_a$s in bovine cytochrome *c* oxidase. Photochem. Photobiol. Sci. 5, 611–620.

[92] Kaila, V.R.I., Verkhovsky, M.I., Hummer, G. and Wikstrom, M. (2008) Glutamic acid 242 is a valve in the proton pump of cytochrome c oxidase. Proc. Natl. Acad. Sci. USA 105, 6255–6259.

[93] Zheng, X., Medvedev, D.M., Swanson, J. and Stuchebrukhov, A.A. (2003) Computer simulation of water in cytochrome *c* oxidase. Biochim. Biophys. Acta 1557, 99–107.

[94] Wikstrom, M., Verkhovsky, M.I. and Hummer, G. (2003) Water-gated mechanism of proton translocation by cytochrome c oxidase. Biochim. Biophys. Acta 45238, 1–5.

[95] Xu, J. and Voth, G.A. (2007) Redox-coupled proton pumping in cytochrome *c* oxidase: Further insights from computer simulation. Biochim. Biophys. Acta 1777, 196–201.

[96] Konstantinov, A.A. (1977) Role of protons in the mechanism of coupling site III of the mitochondrial respiratory chain: Cytochrome oxidase as an electronic-protonic generator of membrane potential. Doklady Akad. Nauk SSSR 237, 713–716.

[97] Iwata, S., Ostermeier, C., Ludwig, B. and Michel, H. (1995) Structure at 2.8 A resolution of cytochrome *c* oxidase from *Paracoccus denitrificans*. Nature 376, 660–669.

[98] Tsukihara, T., Aoyama, H., Yamashita, E., Takashi, T., Yamaguichi, H., Shinzawa-Itoh, K., Nakashima, R., Yaono, R. and Yoshikawa, S. (1996) The whole structure of the 13-subunit oxidized cytochrome *c* oxidase at 2.8 A. Science 272, 1136–1144.

[99] Popovic, D.M. and Stuchebrukhov, A.A. (2004) Electrostatic study of the proton pumping mechanism in bovine heart cytochrome *c* oxidase. J. Am. Chem. Soc. 126, 1858–1871.

[100] Wikstrom, M. (2004) Cytochrome *c* oxidase: 25 years of the elusive proton pump. Biochim. Biophys. Acta 1655, 241–247.

[101] Zaslavsky, D., Sadoski, R.C., Wang, K., Durham, B., Gennis, R.B. and Millett, F. (1998) Single electron reduction of cytochrome *c* oxidase compound F: Resolution of partial steps by transient spectroscopy. Biochemistry 37, 14910–14916.

[102] Sadoski, R.C., Zaslavsky, D., Gennis, R.B., Durham, B. and Millett, F. (2001) Exposure of bovine cytochrome *c* oxidase to high Triton X-100 or to alkaline conditions causes a dramatic change in the rate of reduction of compound F. J. Biol. Chem. 276, 33616–33620.

[103] Zaslavsky, D., Sadoski, R.C., Rajagukguk, S., Geren, L., Millett, F., Durham, B. and Gennis, R.B. (2004) Direct measurement of proton release by cytochrome *c* oxidase in solution during the F-O transition. Proc. Natl. Acad. Sci. USA 101, 10544–10547.

[104] Sugitani, R. and Stuchebrukhov, A.A. (2009) Molecular dynamics simulation of water in cytochrome c oxidase reveals two water exit pathways and the mechanism of transport. Biochim. Biophys. Acta 1787, 1140–1150.

[105] Salomonsson, L., Faxen, K., Adelroth, P. and Brzezinski, P. (2005) The timing of proton migration in membrane-reconstituted cytochrome c oxidase. Proc. Natl. Acad. Sci. USA 102, 17624–17629.

[106] Rich, P.R. (1995) Towards an understanding of the chemistry of oxygen reduction and proton translocation in the iron-copper respiratory oxidases. Aust. J. Plant Physiol. 22, 479–486.

[107] Quenneville, J., Popovic, D.M. and Stuchebrukhov, A.A. (2006) Combined DFT and electrostatics study of the proton pumping mechanism in cytochrome *c* oxidase. Biochim. Biophys. Acta 1757, 1035–1046.

[108] Nagano, S. and Poulos, T.L. (2005) Crystallographic study on the dioxygen complex of wild-type and mutant cytochrome P450cam. J. Biol. Chem. 280, 31659–31663.

[109] Blomberg, M., Siegbahn, P.E.M., Babcock, G.T. and Wikstrom, M. (2000) O–O bond splitting mechanism in cytochrome oxidase. J. Inorg. Chem. 80, 1238–1243.